Semiempirical Molecular Orbital Study on the Transition States for the *anti*-Selective Michael Addition Reactions of the Lithium *Z*-Enolates of *N*-Alkylideneglycinates to α,β-Unsaturated Esters

Akira Tatsukawa,[a] Keiko Kawatake,[a] Shuji Kanemasa[b] and Jerzy M. Rudziński[c]
[a] *Department of Chemistry, Faculty of Science, Kochi University, Akebono-cho, Kochi 780, Japan*
[b] *Institute of Advanced Material Study, Kyushu University, Kasugakoen, Kasuga 816, Japan*
[c] *Fujitsu Kyushu System (FQS) Ltd., Hakata Eki Mae 1-5-1, Hakata-ku, Fukuoka 812, Japan*

Semiempirical molecular orbital calculations (MNDO and PM3) show that the lithium *Z*-enolates derived from *N*-alkylideneglycinates react with α,β-unsaturated esters through a stepwise mechanism *via* the intermediate formation of Michael adducts. The initial step involves an *anti*-selective carbon–carbon bond formation through a Michael addition process and the second step consists of stereoselective ring formation or a 1,3-dipolar cycloaddition. The energy difference between the transition states for each step depends upon the steric hindrance caused by the alkylidene moiety: bulky alkylidene substituents prefer the formation of Michael adducts and small ones prefer 1,3-dipolar cycloadducts. The exclusively high *anti*-selectivity observed in the Michael addition step is due to the attractive molecular orbital interaction working between the imine moiety of donor molecules and the α-carbon of the acceptors.

It is known that lithiation of *N*-alkylideneglycinates leads to the selective formation of lithium (*Z*)-enolates. The resulting nucleophiles undergo two characteristic carbon–carbon bond forming reactions, exclusively stereoselective 1,3-dipolar cycloadditions giving pyrrolidine-2,4-dicarboxylates and *anti*-selective Michael additions giving single isomers of glutamates, depending upon the reaction conditions and the nature of alkylidene substituents (Scheme 1).[1,2] For example, methyl *N*-benzylideneglycinate reacts with methyl crotonate in the presence of lithium bromide/1,8-diazabicyclo[5.4.0]undec-7-ene (DBU) to produce a single stereoisomer of the pyrrolidine cycloadduct [eqn. (1)].[1a] Rather lower selectivity is observed when sodium hydride is employed as a base,[1b] and cycloadditions of *N*-titanated azomethine ylides afford different types of cycloadduct, depending upon the structures of dipolarophiles and the reaction temperature.[1c] Methyl *N*-(2,2-dimethylpropylidene)glycinate gives a similar stereoselective cycloadduct when lithiated with lithium diisopropylamide (LDA) under irreversible lithiation conditions and allowed to react with methyl crotonate [eqn. (2)].[2a] On the other hand, the corresponding *anti*-Michael adduct isomer is the only product when the same imine ester is lithiated with lithium bromide–DBU under reversible conditions [eqn. (3)].[2a,b] Pure enantiomers of the imine esters derived from *N*-bornylideneglycinates, even when lithiated under irreversible conditions, undergo exclusively *anti*-selective Michael additions with a diastereofacial selectivity of *lk*-1,4-induction [eqn. (4)].[2c–e]

We previously observed in the reaction of methyl *N*-benzylidenealanate with methyl acrylate that the stereoselective formation of a dipolar cycloadduct was accompanied by a trace of the corresponding Michael adduct.[3] Based on these results, we proposed a new stepwise mechanism for the stereoselective dipolar cycloadditions where an intermediate Michael adduct is involved. The stereochemical outcome observed for both the Michael addition and the dipolar cycloaddition is consistent with the proposed stepwise mechanism.[3] However, we were uncertain about (1) what determines the reaction course, Michael addition or 1,3-dipolar cycloaddition, and (2) why the initial Michael addition step is so exclusively *anti*-selective.

Michael additions between lithium *Z*-enolates and *E*-isomers of α,β-unsaturated carbonyl compounds usually show *anti* selectivity, for which several transition state models have been

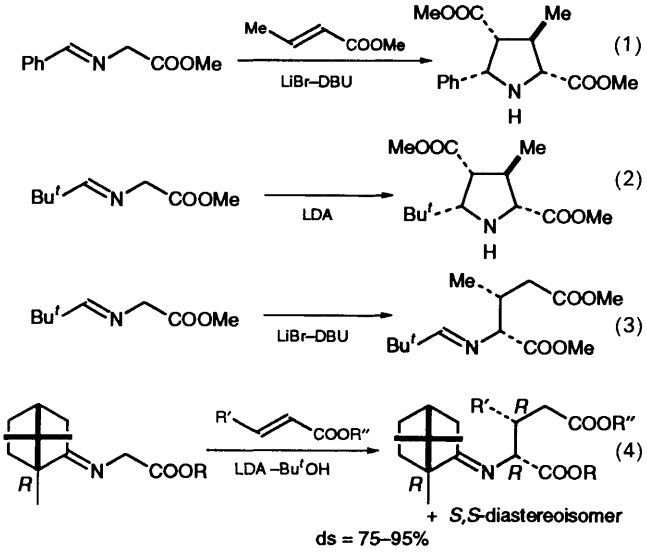

Scheme 1 Stereoselective 1,3-dipolar cycloadditions [eqns. (1), (2)] and *anti*-selective Michael additions [eqns. (3) and (4)] observed in interactions between the lithium *Z*-enolates of *N*-alkylideneglycinates and α,β-unsaturated esters

proposed including the widely accepted Heathcock's chelation model.[4] However, Michael additions of the lithium *Z*-enolates derived from α-hetero-substituted ester and amide derivatives show the opposite stereoselectivity (*syn* selectivity).[5] In particular, reactions of α-alkoxy amides are highly *syn*-selective. Such unusual *syn* selectivity was explained in terms of the position of the lithium ion in the transition state, which is intramolecularly bound to the α-hetero atom. Although the *Z*-enolates of *N*-alkylideneaminoacetates belong to the latter type of enolates, the exclusively high *anti* selectivity cannot be explained by application of an analogous transition state.

To explain the high *anti* stereoselectivity observed in the Michael additions of the lithium enolates of *N*-alkylideneglycinates, we proposed the transition state structure shown in Fig. 1. Here the lithium ion is intramolecularly coordinated with the imine nitrogen and further intermolecularly with the carbonyl oxygen of the acceptor molecule. A carbon–carbon bond is

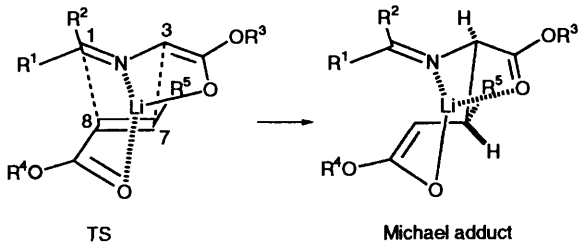

Fig. 1 Transition-state structure previously proposed for the Michael additions of the lithium *Z*-enolates of *N*-alkylideneglycinates with α,β-unsaturated esters

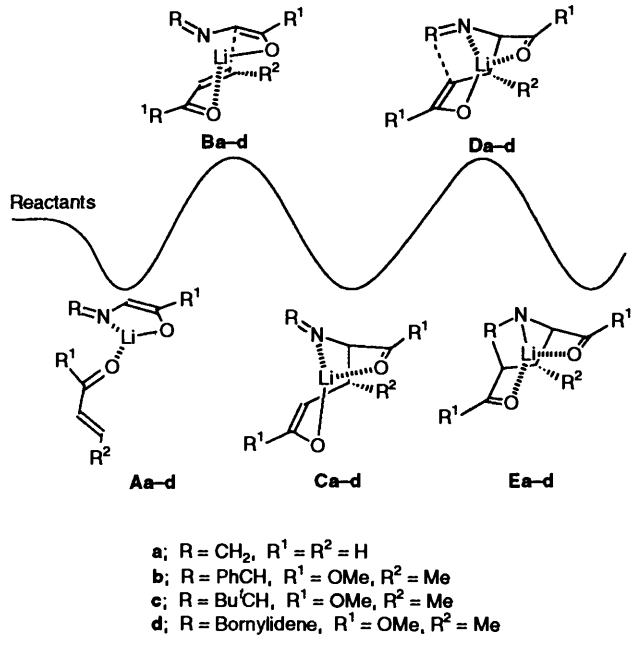

Fig. 2 Reaction pathways of the associative complexes **Aa–d** leading to 1,3-dipolar cycloadducts **Ea–d** *via* Michael adducts **Ca–d**

formed between C3 and C7 under the influence of some attractive molecular orbital interaction working between the imine moiety of the donor enolates and the unsaturated part of the acceptors (C1 and C8). When there is a high degree of steric hindrance around the alkylidene moiety $R^1R^2C=$, further cyclization to dipolar cycloadducts is inhibited.

In the present work, we performed molecular orbital calculations using MNDO and PM3 methods to study the reaction mechanism for the interaction of *Z*-enolates of *N*-alkylideneglycinates with α,β-unsaturated carbonyl acceptors. Several pieces of evidence support our previous proposal of the stepwise reaction mechanism in which lithium *Z*-enolates of *N*-alkylideneglycinates react with α,β-unsaturated carbonyl acceptors leading to 1,3-dipolar cycloadducts *via* intermediate Michael addition products. Two transition-state structures are involved in this reaction mechanism, the initial one being the saddle point leading to the Michael adduct and the second directly connecting the Michael adduct and the 1,3-dipole cycloaddition product (Fig. 2).

Computational Method

Semiempirical molecular orbital methods (MNDO[6] and PM3[7]) implemented in the MOPAC '93[8] program were used throughout this study. ANCHOR II[9] served as a graphic user interface to model the structures, to run the calculations, and to analyse the results. Drawings presented here were drawn with ChemDraw and Chem 3D software. The frontier MO reasoning and the techniques used to study reaction pathways with MO methods are well established and references can be found elsewhere.[10]

Reaction of the lithium *Z*-enolate **2a** of (methyleneamino)-acetaldehyde (**1a**) with propenal (**3**) was chosen as a model system. Calculations were carried out for two types of reaction

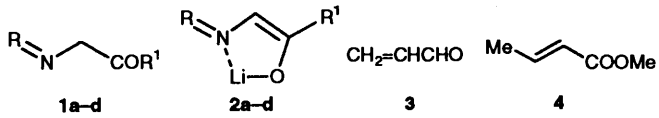

a; R = CH_2, R^1 = H
b; R = PhCH, R^1 = OMe
c; R = But'CH, R^1 = OMe
d; R = Bornylidene, R^1 = OMe

using these substrates. (1) A possible transition state for the concerted cycloaddition reaction between **2a** and **3** was sought by changing the bond distances C3–C7 and C1–C8 (Fig. 1) for a construction in which both bond distances are equal. However, no one-dimensional energy maximum acceptable for the expected transition state was obtained. (2) Accordingly, the *Z*-enolate **2a** and the acceptor **3** were allowed to interact between C3 and C7 and their geometric parameters were adjusted to give the most probable structure for the expected transition state (**Ba** in Fig. 2) in which the distance between C3 and C7 was estimated as 2.1 Å. This transition structure **Ba** leads to either the starting complex **Aa** or the Michael adduct **Ca**. The next calculation started from either the Michael adduct **Ca** or the optimized cyclized product **Ea** to find the transition structure **Da** for the cyclization step, in which the C1–C8 distance was estimated as 2.1 Å. For the calculation of other reactions using **2b–d** and methyl crotonate (**4**), the C3–C7 distance was fixed at about 2.1 Å and the rest of the system was optimized to find the transition state for the Michael addition step. A similar calculation was done to find the transition state for the cyclization step with the fixed distance of 2.1 Å for the C1–C8 bond. The reaction coordinate calculations were done by choosing these distances as a reaction coordinate to locate the best choice for the saddle point. The resulting structures were gradient-optimized, then normal coordinate analyses were performed to check whether they represented true transition states (one negative eigenvalue of the Hessian), and finally both transition state structures (**B** and **D**) were used in the intrinsic reaction coordinate calculation (IRC) to correlate them with the corresponding energy minima.

Results and Discussion

Fig. 2 shows the reaction pathway calculated for the Michael additions between the lithium *Z*-enolates of *N*-alkylideneglycinates and unsaturated carbonyl acceptors (**A** to **C**) and the subsequent cyclization leading to 1,3-dipolar cycloaddition products (**C** to **E**). The starting substrate is represented here as associative complexes (**A**) between the donor and acceptor molecules where the lithium atom coordinates intramolecularly to the imine nitrogen atom (to give a fine-membered ring substructure) and intermolecularly to the carbonyl oxygen of the acceptors. These complex structures were obtained by the IRC calculation from the transition state **B**. It should be emphasized that structures of the initial transition state **B**, the Michael adduct **C**, and the second transition state **D** are very similar to each other, reflecting the subtle geometrical changes when the system undergoes further cyclization leading to the 1,3-dipolar cycloadduct **E** (Fig. 3).

Table 1 MNDO- and PM3-calculated energies (in kcal mol^{-1}) for the transition states and energy minima along the reaction pathway leading to the Michael adduct **C** and the 1,3-dipolar cycloadduct **E**. The potential energies are relative to the energy of reactants, *cf.* Fig. 2

Entry	Substrates	R	R^1	R^2	Method	**B**	**C**	**D**	**E**	$\Delta H_{C\,to\,D}$[a]
1	**2a** + **3**	CH_2	H	H	MNDO	3.7	−16.5	−2.1	−24.6	14.4
2	**2a** + **3**	CH_2	H	H	PM3	2.1	−13.3	−1.7	−18.9	11.6
3	**2b** + **4**	PhCH	OMe	Me	MNDO	19.5	2.3	14.6	−8.6	12.3
4	**2b** + **4**	PhCH	OMe	Me	PM3	8.6	−1.3	7.9	−9.5	9.2
5	**2c** + **4**	Bu^{t}CH	OMe	Me	MNDO	16.4	−2.0	16.0	−2.5	18.0
6	**2c** + **4**	Bu^{t}CH	OMe	Me	PM3	8.1	−3.0	8.4	−6.3	11.4
7	**2d** + **4**	Bornylidene	OMe	Me	MNDO	19.5	1.2	29.7	12.7	28.5
8	**2d** + **4**	Bornylidene	OMe	Me	PM3	7.8	−4.4	12.9	−3.1	17.3

[a] Energy barrier for the cyclization step (kcal mol^{-1}) relative to the energy of the corresponding Michael adduct.

Table 2 PM3-calculated HOMO–LUMO energy differences (eV) and C1–C8 distances (Å) of the Michael adducts **Ca–d** and the energy barriers for the cyclization step (**C** to **D**)

Michael adduct	R	$\Delta E_{HOMO/LUMO}$/eV	d_{C1-C8}/Å	Energy barrier $\Delta H_{C\,to\,D}$/kcal mol^{-1}
Ca	CH_2	7.41[a]	4.261	11.6
Cb	PhCH	6.49	3.185	9.2
Cc	Bu^{t}CH	7.37[a]	3.219	11.4
Cd	Bornylidene	10.10[b]	3.317	17.2

[a] Energy difference from second LUMO to HOMO. [b] Energy difference from second LUMO to second HOMO.

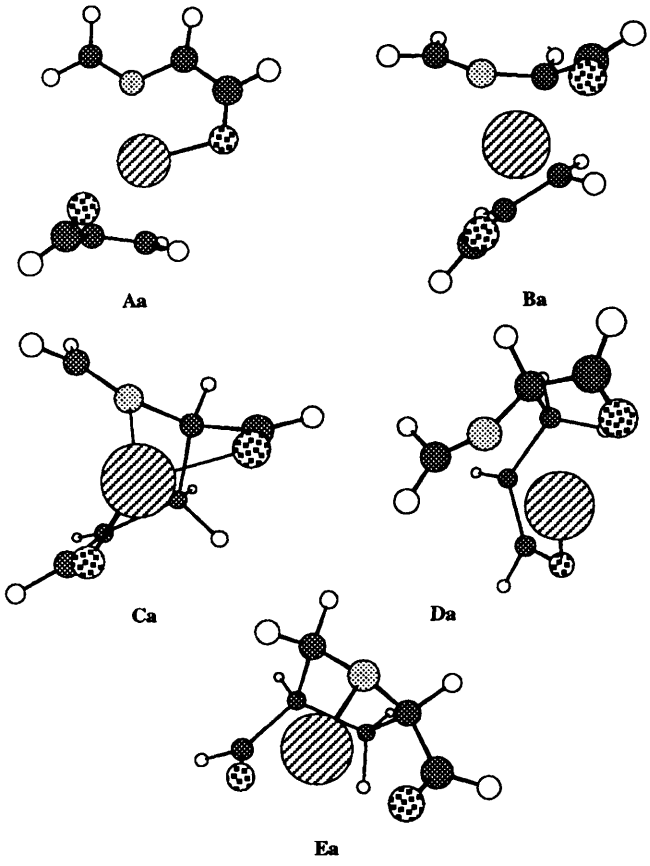

Fig. 3 MNDO-optimized structures of the stationary points on the PES of the stepwise 1,3-dipole cycloaddition reaction of lithium *Z*-enolate **2a** with propenal **3**

In the model system using methyleneaminoacetaldehyde (**1a**) and propenal (**3**), the transition state **Ba** for the Michael addition step leading to Michael adduct **Ca** is higher in energy than that for the cyclization step **Da** leading to the 1,3-dipolar cycloadduct **Ea** (by 5.9 and 3.8 kcal mol^{-1} in MNDO and PM3 calculations, respectively) indicating that the latter cyclization step is thermodynamically controlled in the whole reaction (Fig. 2, entries 1 and 2 of Table 1) and that the types of product depends upon the relative potential energies of **Ca** and **Ea**. Since the 1,3-dipolar cycloadduct **Ea** is much more stabilized than the Michael adduct **Ca**, the reaction between **2a** and **3** goes to the cyclized product **Ea**. Fig. 3 shows the MNDO-optimized structures of the energy minima (**Aa**, **Ca** and **Ea**) and saddle points (**Ba** and **Da**) on this model PES.

Introduction of a phenyl substituent onto the imine carbon atom of the model donor molecule **1a** reduces the energy barrier for the cyclization step. In the model system using **1a**, the cyclization reaction of the Michael adduct **Ca** requires 14.4 or 11.5 kcal mol^{-1} of activation energy in the MNDO or PM3 calculation (**Ca** to **Da**), respectively, while in the case of methyl *N*-benzylideneglycinate (**1b**) the barrier amounts to 12.4 (MNDO) or 9.2 kcal mol^{-1} (PM3) (**Cb** to **Db**, entries 3 and 4 of Table 2). In this case also, the cyclized product **Eb** is thermodynamically more stable and the energy barrier for the cyclization step is lower than that for the Michael-addition step. Accordingly, the reaction of **2b** with **4** leads to the preferred formation of the 1,3-dipolar cycloadduct **Eb** as a thermodynamically controlled product.

On the other hand, when a donor molecule carries a sterically hindered substituent as seen in **1d**, the cyclization step becomes difficult compared with the Michael-addition step (**Bd** *vs.* **Dd**). The energy barrier for the cyclization step (**Cd** to **Dd**) in the reaction of methyl *N*-bornylideneglycinate (**1d**) with methyl crotonate (**4**) is as big as 28.5 according to MNDO or 17.2 kcal mol^{-1} to PM3 calculations. In addition, the cycloadduct **Ed** is less stable than the corresponding Michael adduct **Cd**, and hence the cyclization reaction of the Michael adduct **Cd** is endothermic. Therefore, the product expected to form in this reaction is the kinetically controlled Michael adduct **Cd**, and this is in fact observed.

In the reaction of the *tert*-butyl-substituted imine ester **1c**, also sterically hindered, the Michael addition and cyclization steps have comparable energy barriers (entries 5 and 6 in Table 1), and the Michael adduct **Cc** and the cyclized product **Ec** show almost the same thermodynamic stabilities. Accordingly, this

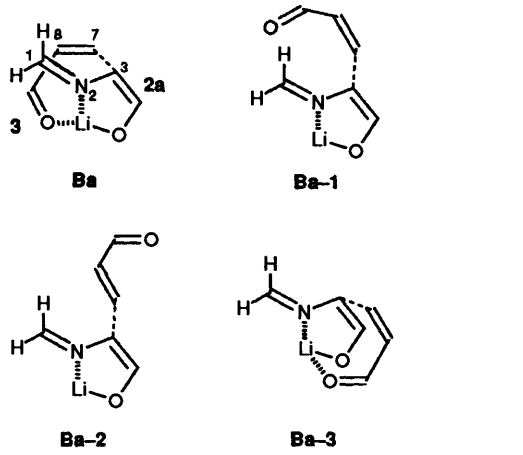

	$\Delta H^{\ddagger}$/kcal mol^{-1}	ΔH/kcal mol^{-1}
Ba	2.06	−13.25
Ba-1	25.36	17.84
Ba-2	25.81	17.47
Ba-3	3.31	−13.29

Fig. 4 A variety of transition-state structures calculated by using PM3 parameters for the model Michael addition between the lithium enolate **2a** and acceptor **3**. $\Delta H^{\ddagger}$ and ΔH represent the energy barrier and the heat of the reaction on going from the reactants to the Michael adduct, respectively.

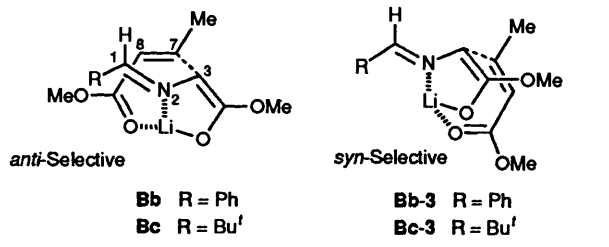

Bb R = Ph
Bc R = Bu^t

Bb-3 R = Ph
Bc-3 R = Bu^t

	$\Delta H^{\ddagger}$/kcal mol^{-1}	ΔH/kcal mol^{-1}
Bb	8.63	−1.31
Bb-3	9.66	−1.46
Bc	8.07	−3.02
Bc-3	8.31	−3.69

Fig. 5 PM3-calculated transition-state structures **Bb**, **c** and **Bb**, **c-3** leading to *anti*- and *syn*-adducts, respectively; *anti*-selective reactions are more favoured

reaction gives rise to either Michael adduct **Cc** or cyclized product **Ec**, depending upon the reaction conditions.

On the basis of these computational data, we can now answer the first question of what determines the reaction types, Michael addition or 1,3-dipolar cycloaddition, in reactions of the lithium enolates **2b–d** derived from alkylideneglycinates **1b–d** with a crotonate acceptor **4**. The Michael addition and the dipolar cycloaddition steps are not based on the separated reaction paths but are closely related to each other. The Michael-addition step is followed by the 1,3-dipolar cycloaddition step so that both reactions show common stereoselectivities. The reaction of sterically less hindered methyl *N*-benzylideneglycinate (**1b**) with methyl crotonate (**4**) leads only to the 1,3-dipolar cycloadduct **Eb**, and bulky methyl *N*-bornylideneglycinate (**1d**) gives only the Michael adduct **Ed**.

The above discussion of the stabilities of Michael adducts and cycloadducts is based on the enthalpy differences as they evolve from these semiempirical calculations, and certainly that is not the whole picture. One should also mention entropic contributions to the thermodynamic stabilities. The PM3 calculated entropy change going from the Michael adduct (**C**) to the cycloadduct (**E**) (refer to Fig. 2 and Table 1) is negative ($-T\Delta S$ = 0.52 kcal mol^{-1} at 298 K) in the model system (*a*) and positive in all other calculated reactions: $-T\Delta S$ = −0.25, −1.02, −0.90 kcal mol^{-1} for **b**, **c** and **d**, respectively. This means that, except for the model system, the entropy change favours the cycloadducts. In the extreme cases the entropic contributions amount to about 1 kcal mol^{-1} at the most and therefore this does not change our conclusion. It should be noted that the entropic contributions given above should be treated with caution: they are valid subject to the accuracy of the vibrational frequencies obtained by semiempirical methods which have been parametrized to reproduce experimental heats of formation and not vibrational frequencies.

Since structural differences in the common portions of the transition-state structures **Da–d** for the cyclization step looked negligible, we analysed the frontier molecular orbital of each Michael adduct **Ca–d**. Energy differences between the highest occupied molecular orbital (HOMO) and the lowest unoccupied molecular orbital (LUMO) or between the HOMO and the second lowest unoccupied molecular orbital (SLUMO), depending upon the matching of the phase of HOMO at C8 and LUMO or SLUMO at C1 are given in Table 2. Energy barriers for the cyclization step (**Ca–d** to **Da–d**) obtained in the PM3 calculation are also listed in Table 2. Introduction of a phenyl substituent reduces the energy difference between HOMO and LUMO and the distance between C1 and C8 is the shortest of all Michael adducts **Ca–d**, indicating that the cyclization step from the Michael adduct **Cb** is easier than any other reactions. The bornylidene and 2,2-dimethylpropylidene substituents increase the energy gaps between the HOMO and LUMO and both reaction sites C1 and C8 are too remote to form a new bond. A steric effect is apparently the major reason.

With optimized structures of the cyclized products **Ea–d** in hand, the saddle-point calculation was performed in order to find the transition-state structures for the concerted 1,3-dipolar cycloadditions. However, the transition states obtained by this PM3 calculation are just the same as those calculated for the Michael-addition step. This will be discussed later.

It is now concluded that the stereoselectivity observed in the 1,3-dipolar cycloadditions of lithium enolates **2a–d** with crotonate **4** must reflect that of the initial Michael addition step. Why, then, was the Michael addition step (**A** to **C** *via* transition state **B**) so exclusively *anti*-selective? To solve this problem, we first of all looked for other possible transition-state structures for the Michael-addition step in the model system (other stereoisomeric routes equivalent to the transformation of **Aa** into **Ca**). Thus, new reaction coordinate pathways were calculated by changing the dihedral angle ∠N2–C3–C7–C8 of **Ba** to reach another energy minimum, and then transition structure **Ba–1** was obtained after structure optimization (Fig. 4). Exchange of the formyl and hydrogen groups of **Ba-1** led to **Ba-2** after optimization. A similar procedure starting from **Ba-2** provided **Ba-3**, and these four were all the calculated transition states. Among them, **Ba-1** and **Ba-2** are much less stable than the other two **Ba** and **Ba-3**, indicating that coordination of the lithium atom to the acceptor carbonyl oxygen is essential to stabilize the transition energy. Although an energy difference of 1.25 kcal mol^{-1} is very small, the transition structure **Ba** is concluded to be the most stable transition state.

In the calculations of similar reactions using the lithium *Z*-enolates **2b**, **c** derived from *N*-alkylideneglycinates **1b**, **c** and methyl crotonate (**4**), each of the two transition states **Bb**/**Bb-3** and **Bc**/**Bc-3** were obtained, transition states **Bb**, **c** leading to *anti*-Michael adducts **Eb**, **c** and **Bb-3**, **c-3** *syn*-stereoisomers. Transition states **Bb**, **c** were again more stable than **Bb-3**, **c-3**

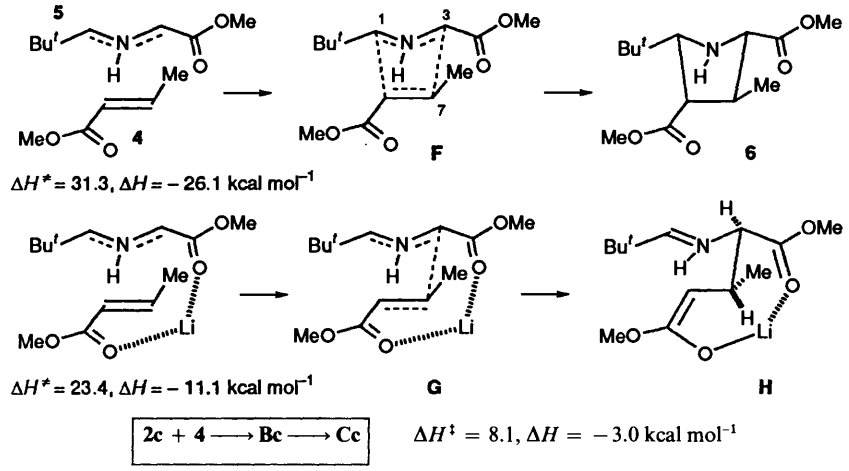

Fig. 6 PM3 calculation shows that *N*-protonated azomethine ylide **5** undergoes a stereoselective cycloaddition to methyl crotonate **4** leading to **6**, while Michael addition takes place in the presence of a lithium ion leading to **H**

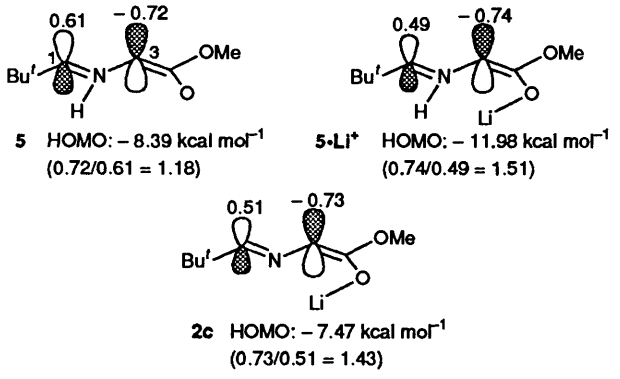

Fig. 7 HOMO levels and orbital coefficients of donor molecules *N*-protonated azomethine ylide **5**, its lithiated species **5**·Li^+, and lithium enolate **2c**

(Fig. 5). Thus, the calculation results are consistent with the experimental data that the Michael-addition step proceeds in an *anti*-selective manner.

An interesting result was provided by PM3 calculation for the reaction of the *N*-protonated azomethine ylide **5** with methyl crotonate (**4**). This reaction takes place, according to calculation, in a concerted manner *via* transition state **F** leading to cycloadduct **6** (Fig. 6) where the activation energy is 31.3 kcal mol^{-1}. On the other hand, the same reaction is accelerated in the presence of a lithium ion (activation energy 23.4 kcal mol^{-1}) and the calculated product is not the cycloadduct but the Michael adduct **H**. It was already mentioned above that the reaction of the lithium enolate **2c** with crotonate **4** led to the Michael adduct **Cc** *via* transition state **Bc** (activation energy 8.1 kcal mol^{-1}).

In the concerted 1,3-dipolar cycloaddition path of the *N*-protonated azomethine ylide **5**, the orbital interactions must operate comparably both between C3/C7 and C1/C8 in the transition state **F**. The interaction between C3/C7 becomes more favoured in the presence of a lithium ion and the formation of the Michael addition product **H** becomes predominant. However, in this case also, there should be some orbital interaction between C1/C8. Accordingly, it is very likely that such an attractive interaction also occurs in the reaction of lithium enolate **2c** with **4**.

Fig. 7 shows the energy levels of the highest occupied molecular orbital (HOMO) and orbital coefficients at C1 and C3 of donor molecules, such as *N*-protonated azomethine ylide **5**, its lithium ion-coordinating *N*-protonated azomethine ylide **5**·Li^+, and lithium enolate **2c**. The coefficient ratios C3/C1 between C3 and C1 of HOMO of these donor molecules decrease from 1.18 (**5**) to 1.43 (**2c**), and lithium enolate **2c** and metal-coordinated ylide **5**·Li^+ (ratio: 1.51) show very close ratios. It is interesting that such a small difference in molecular coefficients leads to different reaction paths, 1,3-dipolar cycloaddition or Michael addition.

As a result, some sort of molecular orbital interaction must be operative between C1/C8 in the transition state for the reaction of lithium enolates **2** with α,β-unsaturated esters **4**. This is a main reason why the Michael addition step is exclusively *anti*-selective. From the steric viewpoint, the transition state **Bb-3**, **c-3** leading to *syn*-Michael adducts (Fig. 5) looks more favourable than the transition state **Bb**, **c** leading to *anti*-adducts, especially when the enolates **2** carry a bulky substituent (R) on the imine carbon. Nevertheless such an attractive molecular orbital interaction counterbalances the steric interaction.

Acknowledgements

This work was partially supported by the Sasakawa Scientific Research Grant from The Japan Science Society (A. T.). We also thank Mr. Masanori Ohmura of FQS for his help in the computer system set-up.

References

1 (*a*) O. Tsuge, S. Kanemasa and M. Yoshioka, *J. Org. Chem.*, 1988, **53**, 1384; (*b*) S. Kanemasa, M. Yoshioka and O. Tsuge, *Bull. Chem. Soc. Jpn.*, 1989, **62**, 2196; (*c*) S. Kanemasa, O. Uchida, E. Wada and H. Yamamoto, *Chem. Lett.*, 1990, 105; (*d*) S. Kanemasa and H. Yamamoto, *Tetrahedron Lett.*, 1990, **31**, 3633; (*e*) S. Kanemasa, H. Yamamoto, E. Wada, T. Sakurai and K. Urushido, *Bull. Chem. Soc. Jpn.*, 1990, **63**, 2857; (*f*) S. Kanemasa, T. Hayashi, J. Tanaka, H. Yamamoto and T. Sakurai, *J. Org. Chem.*, 1991, **56**, 4473; (*g*) S. Kanemasa, M. Yoshioka and O. Tsuge, *Bull. Chem. Soc. Jpn.*, 1989, **62**, 869; (*h*) S. Kanemasa, T. Hayashi, H. Yamamoto, E. Wada and T. Sakurai, *Bull. Chem. Soc. Jpn.*, 1991, **64**, 3274; (*i*) D. A. Barr, R. Grigg, H. Q. N. Gunaratne, J. Kemp, P. McMeekin and V. Sridharan, *Tetrahedron*, 1988, **44**, 557; (*j*) D. A. Barr, R. Grigg and V. Sridharan, *Tetrahedron Lett.*, 1989, **30**, 4727; (*k*) D. A. Barr, M. J. Dorrity, R. Grigg, J. F. Malone, J. F. Montgomery, S. Rajviroongit and P. Stevenson, *Tetrahedron Lett.*, 1990, **31**, 6569; (*l*) R. Annunziata, M. Cinquini, F. Cozzi, L. Raimondi and T. Pilati, *Tetrahedron Asym.*, 1991, **2**, 1329; (*m*) T. Coulter, R. Grigg, J. F. Malone and V. Sridharan, *Tetrahedron Lett.*, 1991, **32**, 5417; (*n*) P. Allway and R. Grigg, *Tetrahedron Lett.*, 1991, **32**, 5817.

2 (*a*) S. Kanemasa, O. Uchida and E. Wada, *J. Org. Chem.*, 1990, **55**, 4411; (*b*) H. Yamamoto, S. Kanemasa and E. Wada, *Bull. Chem. Soc. Jpn.*, 1991, **64**, 2739; (*c*) S. Kanemasa, A. Tatsukawa, E. Wada and O. Tsuge, *Chem. Lett.*, 1989, 1301; (*d*) S. Kanemasa, A. Tatsukawa and E. Wada, *J. Org. Chem.*, 1991, **56**, 2875; (*e*) A. Tatsukawa,

M. Dan, M. Ohbatake, K. Kawatake, T. Fukata, E. Wada, S. Kanemasa and S. Kakei, *J. Org. Chem.*, 1993, **58**, 4221.
3 S. Kanemasa, M. Yoshioka and O. Tsuge, *Bull. Chem. Soc. Jpn.*, 1989, **62**, 869.
4 Linear transition state model: (*a*) C. H. Heathcock, M. H. Norman and D. E. Uehling, *J. Am. Chem. Soc.*, 1985, **107**, 2797; (*b*) C. H. Heathcock and D. A. Oara, *J. Org. Chem.*, 1985, **50**, 3022; (*c*) M. Yamaguchi, K. Hasebe, S. Tanaka and T. Minami, *Tetrahedron Lett.*, 1986, **27**, 959; coordination transition state model: (*d*) E. J. Corey and R. T. Peterson, *Tetrahedron Lett.*, 1985, **26**, 5025; (*e*) K. Tomioka, K. Yasuda and K. Koga, *Tetrahedron Lett.*, 1986, **27**, 4611; (*f*) D. A. Oare, M. A. Henderson, M. A. Sanner and C. H. Heathcock, *J. Org. Chem.*, 1990, **55**, 132; (*g*) K. Busch, U. M. Groth, W. Kühnle and U. Schöllkopf, *Tetrahedron*, 1992, **48**, 5607.
5 (*a*) S. Kanemasa, M. Nomura and E. Wada, *Chem. Lett.*, 1991, 1735; (*b*) S. Kanemasa, M. Nomura and Y. Taguchi, *Chem. Lett.*, 1992, 1801.
6 (*a*) M. J. S. Dewar and W. Thiel, *J. Am. Chem. Soc.*, 1977, **99**, 4899; (*b*) MNDO Lithium parameters from MNDOC by W. Thiel, *QCPE*, Program No. 438, Vol. 2, p. 63, 1982.
7 (*a*) J. J. P. Stewart, *J. Comput. Chem.*, 1989, **10**, 209; (*b*) PM3 lithium parameters: E. Anders, R. Koch and P. Freunscht, *J. Comput. Chem.*, 1993, **14**, 1301.
8 MOPAC 93, J. J. P. Stewart and Fujitsu Ltd, Tokyo, Japan, 1993.
9 ANCHOR II™, a molecular design support system for SUN™ computers developed by FUJITSU Ltd. and Kureha Chemical Industry, Co. Ltd., 1992.
10 (*a*) I. Fleming, *Frontier Orbitals and Organic Chemical Reactions*, Wiley, Chichester, 1978; (*b*) M. L. McKee and M. Page, 'Computing Reaction Pathways on Molecular Potential Energy Surfaces', in *Reviews in Computational Chemistry*, Vol. 4, eds. K. B. Lipkowitz and D. B. Boyd, VCH, New York, 1993.

Paper 4/03764B
Received 21*st June* 1994
Accepted 3*rd August* 1994